Chapter

Assessing Seismic Site Response at Areas Characterized by a Thick Buried Low-Velocity Layer

Daniela Farrugia, Pauline Galea and Sebastiano D'Amico

Abstract

Earthquake ground motion is dependent on various factors, including local ground conditions. Whilst many studies have characterized the effect of having outcropping "soft" geological layers which have the ability to amplify ground motion, there is minimal literature on the effect of having such layers embedded between two harder layers. This situation creates a seismic wave velocity inversion. The Maltese islands (Central Mediterranean) present a good opportunity for the study of velocity inversion as almost half of the islands are characterized by a thick buried layer of clay. The results presented in this chapter are a combination of studies which have been conducted on the Maltese islands, using non-invasive geophysical prospecting techniques in areas characterized by a thick buried low-velocity layer, to characterize the response of earthquake ground shaking in such geological situations.

Keywords: low-velocity layers, site response analysis, shear-wave velocity profiling, V_{S30}, seismic building codes

1. Introduction

It is presently well-established that earthquake ground shaking at a particular site is a function of a set of physical parameters and phenomena including the soil conditions beneath the site. Sites characterized by geological layers with a significant impedance contrast are prone to increasing the amplitude of ground motion, changing the frequency content and also lengthening the duration of the earthquake.

Various studies have investigated the effect of outcropping soft geological layers on earthquake ground motion both experimentally and theoretically [1–4]. However, whilst it is usually assumed that the shear-wave velocity (V_S) increases with depth, soft geological layers with low-velocity "sandwiched" between higher velocity layers can also be present. Such situations create what is known as a velocity inversion.

The presence of a buried thick low-velocity layer is not uncommon, especially in sedimentary environments encompassing clay deposits. However, the effects of such stratigraphies on site effects are not often studied or documented. Moreover, seismic building codes such as the Eurocode 8 (EC8), suggest the use of the average shear-wave velocity in the upper 30 m (V_{S30}) to classify sites in different categories.

Hypothetically this approach is not viable for sites characterised by buried low-velocity layers because the first 30 m could be characterised by high velocity geological material.

The Maltese islands (Central Mediterranean) present the perfect case for studying the effect of buried low-velocity layers. The islands are characterised by a four-layer sequence of limestones and clays [5] (**Figure 1**). While the eastern half of the archipelago is characterised by limestone layers, the western half exhibits limestone plateaux and hillcaps, ranging in thickness from thickness from 2 m up 162 m, covering a clay layer which can be up to 75 m thick [6].

The research presented in this chapter was motivated by the following problems related to the Maltese islands:

- the lack of information about average V_S values of different lithotypes making up the Maltese islands;
- the lack of site response studies on a national scale;
- the lack of knowledge about the effect of the buried clay on site response;
- the V_{S30} might not be the right proxy for site response;
- the lack of a national annex for the Eurocode8.

Even though this study is based and intended for the Maltese islands, results from it can still shed light on the effect of low-velocity layers in any context globally. To tackle the above-mentioned issues, a two-fold process was taken: firstly V_S profiles were obtained using ambient-noise techniques at various sites around

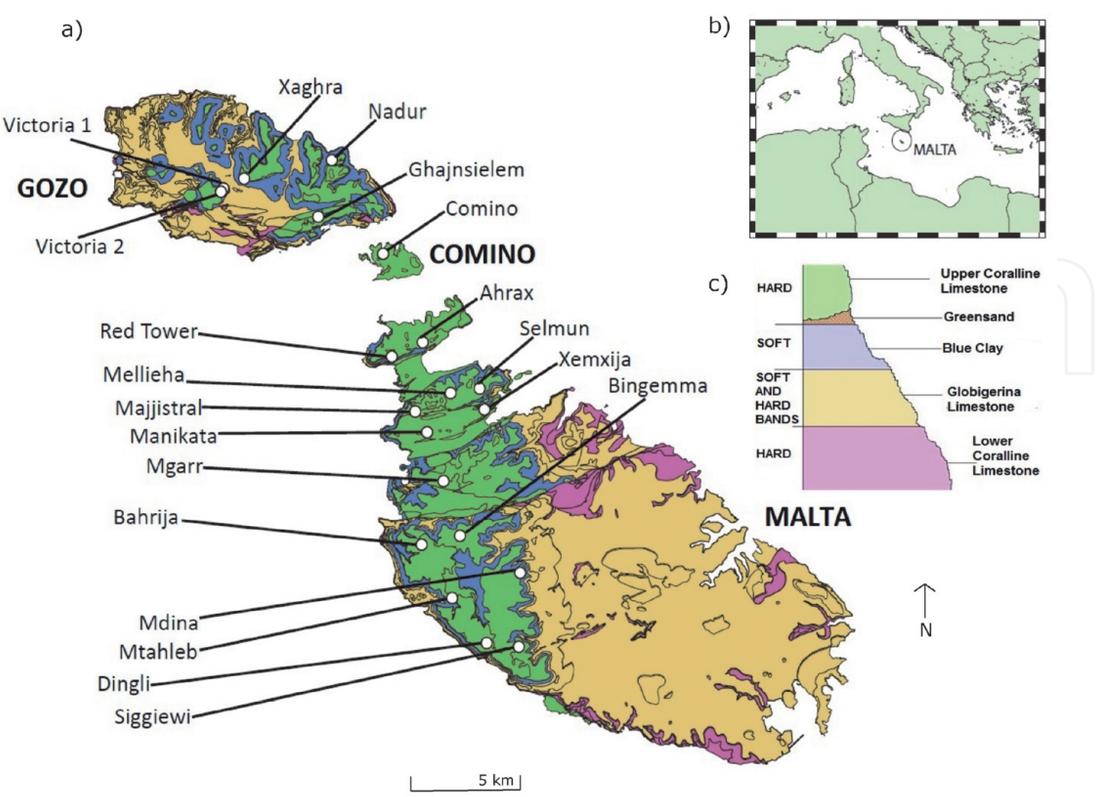

Figure 1.
(a) A geological map of the Maltese islands with the location of the studied sites; (b) the location of the Maltese islands in the Central Mediterranean; (c) schematic showing the geological formations of the Maltese islands.

the islands characterised by buried clay and secondly, these profiles were used as an input to the equivalent-linear site response analysis programme SHAKE2000 to determine the site response.

2. The geology of the Maltese islands

The Maltese archipelago, which consists of three main islands (Malta, Gozo and Comino) and covers an area of around 316 km^2, was formed as marine sediments during the Oligocene and Miocene epochs. The islands lie in the Sicily Channel (**Figure 1b**) on a relatively stable plateau of the African foreland, known as the Pelagian Platform, about 200 km south of the convergent segment of the Europe-Africa plate boundary that runs through Sicily.

Geologically, the islands are made up of four main strata of lime-rich sedimentary rocks, with the composition and texture of each layer depending among other things, on the grain size of the sediment and depth of deposition [7]. Starting from the oldest and the bottom-most layer, the formations are: the Lower Coralline Limestone (LCL), the Globigerina Limestone (GL), the Blue Clay (BC) and the Upper Coralline Limestone (UCL) (**Figure 1c**).

The compact LCL forms most of Malta's southern and south-western coastline along with some inland outcrops associated with faults. The base of the LCL cannot be seen above sea-level and it is exposed through a thickness of up to 140 m. It is non-homogeneous and composed of five different 'facies' according to depositional environment of the sediments [7, 8]. The GL covers large areas of central and southern Malta and Gozo [9]. It is a chalky and soft yellowish fine-grained limestone, which is further subdivided into three layers separated by two thin hardground conglomerate layers. Its thickness can vary from as little as 20 m to over 200 m [5].

The BC layer is the softest in the layer package making it easily erodible. It is mostly found beneath the UCL which is the youngest of the layers. The latter can have variable characteristics, ranging from fractured and friable to highly compact. These two formations are absent in the central and eastern parts of Malta, whereas the western half of Malta and some areas in Gozo retain the full sedimentary sequence. In limited areas, on the uppermost part of the BC layer, one can find a thin layer (between 1 m and 11 m), known as Greensand Formation which is made up of bioclastic limestones rich in the mineral glauconite.

3. Derivation of shear-wave velocities in Maltese rocks using joint inversion of H/V and ESAC curves

Twenty sites have been chosen for this investigation (14 in Malta, 5 in Gozo and 1 in Comino, shown in **Figure 1a**), all of which are characterised by the full sedimentary sequence i.e. the Blue Clay is embedded between the Upper Coralline Limestone above and the Globigerina Limestone below. Since the sites all have similar stratigraphy, any spatial geophysical variations within a particular stratum can also be investigated.

At each site, single-station ambient noise measurements were conducted jointly with geophone array measurements. The sites were chosen not to have any major topographical slopes or irregularities so as to fulfil the 1-D assumption of the array methods. For reasons of clarity, the more detailed results in the next sub-sections are presented only for eight representative sites with a range of stratigraphical characteristics.

3.1 Single-station measurements

Single-station measurements were used to obtain the Horizontal-to-Vertical Spectral Ratio (H/V) for ambient seismic noise. The H/V curve is known to give a peak that matches the S-wave resonance frequency of a site, f_0, which is linked to the S-wave velocity (V_S) of the sedimentary layer and its thickness H by:

$$f_0 = \frac{V_s}{4H}$$

Time-series of 20 minutes each, sampled at 128 Hz, were recorded using the Micromed Tromino™ and analysed using the software Grilla™ to obtain H/V curves in the frequency range of 0.5–64 Hz. The time-series were divided into 60 non-overlapping windows, each 20 s long, as suggested by the SESAME guidelines [10]. Before the analysis, windows which contain any spurious signals were removed to reduce the standard deviation. The H/V curve was obtained by averaging the horizontal spectra using the geometric mean and dividing the mean by the vertical spectrum for each time window. The curves for each window were then averaged to get the final H/V curve [11].

Figure 2 shows the H/V curves obtained at eight representative sites. All curves exhibit a peak between 1 and 2 Hz, the amplitude of which varies between 2 and 5. Previous studies utilising H/V analysis in such areas have also obtained this peak [12–15], which is presumably associated with the boundary separating the BC and the GL [16]. This peak is immediately followed by a drop below 1 in the H/V spectrum over a wide frequency range. This feature has been attributed to the presence of a buried low-velocity layer by [17, 18] and is also evident and consistent in all previous studies of areas of similar lithostratigraphy on the islands.

3.2 Array measurements

The passive seismic array measurements were conducted using Micromed SoilSpy Rosina™ seismic digital acquisition system equipped with 4.5 Hz vertical geophones. The noise signals detected are interpreted as plane Rayleigh waves in their fundamental and higher propagation modes. The number of geophones used varied between 17 and 42 which were placed either in an L- or C-shaped configuration with a regular interstation distance of 5 m, for the majority of the cases. This decision depended on the space available and the expected thickness of the shallow layers. On average the total length of the array was around 150 m and the depth of exploration exceeded 100 m only at a couple of locations. The recordings, each 20 minutes long and sampled at 256 Hz, were analysed using the Extended Spatial

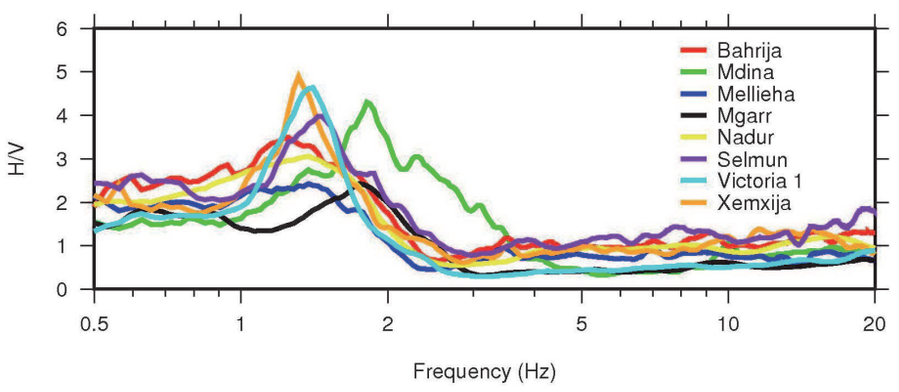

Figure 2.
The H/V curves obtained at eight of the investigated sites.

Auto-Correlation (ESAC) technique and the curves automatically picked by the provided code [19–22].

The ESAC method outputs an effective (or apparent) dispersion curve which in the presence of higher modes, will include a combination of the dispersion curves relative to the relevant modal components [23]. The results for the eight chosen sites are shown in **Figure 3**.

The curves, except in the Mellieha case, exhibit "normal" dispersion characteristics in the low frequency range whereby the effective Rayleigh-wave phase velocity decreases with increasing frequency. At higher frequencies, this trend changes to an inversely dispersive one. This represents an increase in velocity with increasing frequency or decreasing depth. This shape of the effective curves is indicative of the presence of higher modes of surface waves and has been attributed to the presence of a stiff layer overlying a softer one (i.e. UCL and BC, in this case) by various authors (e.g. [23, 24]). In Mellieha, only an inversely dispersive curve was obtained suggesting that the combined thickness of the UCL and BC layers is too high for the GL to be adequately sampled with the given array configuration.

3.3 Data inversion

The H/V and effective dispersion curves were jointly inverted using a Genetic Algorithm (GA; [25]) approach to obtain one-dimensional V_S profiles. The range of allowed values of the most important parameters in the inversion, namely layer thickness and shear-wave velocity, for each site inversion were guided by previous knowledge of the site geology, from geological maps or previous publications. However, the shear-wave velocity in each layer was allowed to vary over a wide range of values, and no indication of where the low-velocity layer is found was given. This was done to assess the ability of the GA to correctly identify and characterize the shear-wave velocity inversion. Up to 10 higher modes were taken into account.

Initially 100 models were randomly generated on which genetic operators (cross-over, mutation and elite selection) are applied for the selection and creation of a second generation of models. The processes were repeated through 150 iterations. For each site, ten separate inversions were run outputting 10 different best-fitting profiles, one from each inversion run. The one profile with the least misfit value from the best 10 profiles was then chosen as the representative profile for the site. The other 9 profiles are useful to estimate the variability and robustness of the final result. **Figures 4** and **5** shows the results of the joint inversion for the eight sites. The V_{S30} was also calculated for each site and is displayed in the figure.

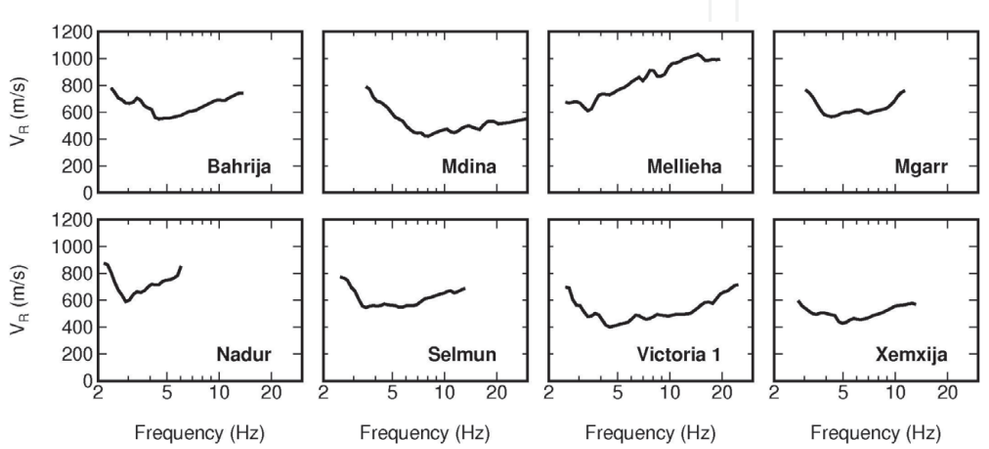

Figure 3.
The effective dispersion curves (Rayleigh-wave vs. frequency) obtained at eight of the investigated sites.

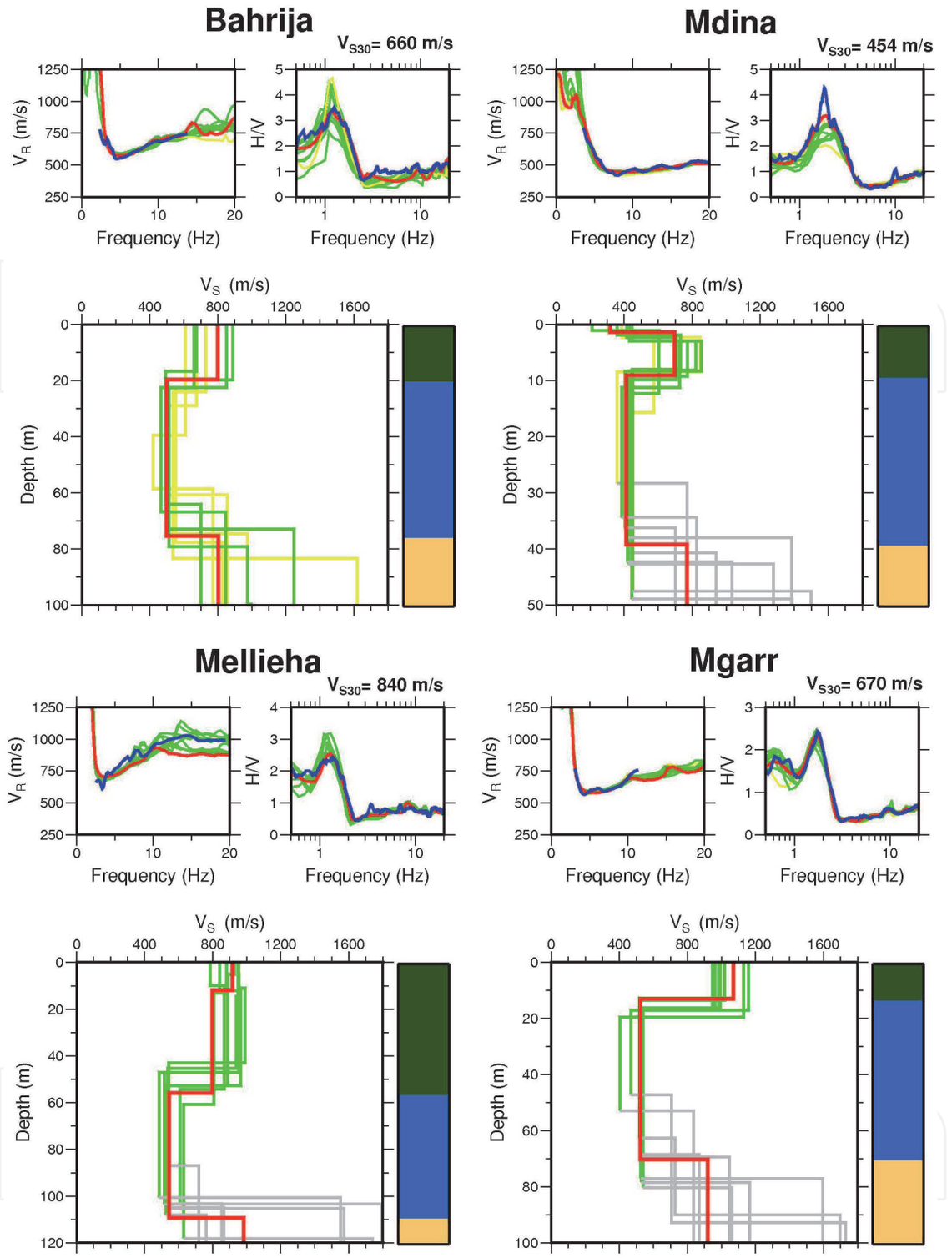

Figure 4.
*The joint inversion results and stratigraphic interpretation (lower panel) for Bahrija, Mdina, Mellieha and Mgarr sites. For each site, the best profiles from each of the 10 inversions are shown, with the red profile representing the one with the lowest misfit. The profiles in green are those characterized by a misfit which is within 50% of the best model's misfit value; the yellow ones are characterized by a misfit greater than 150% of the best model's misfit value. The GL layers are displayed in grey since the values are not reliably constrained by the data. Shown in the upper panel for each site are (from left to right) the effective dispersion and H/V curves. The blue curve is the experimental curve, the red curve shows the best-fitting theoretical curve while the rest (green and yellow) correspond to the other nine profiles. The calculated VS30 for each site is displayed in the top right corner. The colours used in the stratigraphic interpretation correspond to the colours in the geological map (**Figure 1**) [11].*

In general a good match between the theoretical and experimental effective dispersion curves and H/V peak can be observed in all cases. A significantly important feature is that all the final 10 profiles for each site, are in agreement on both the

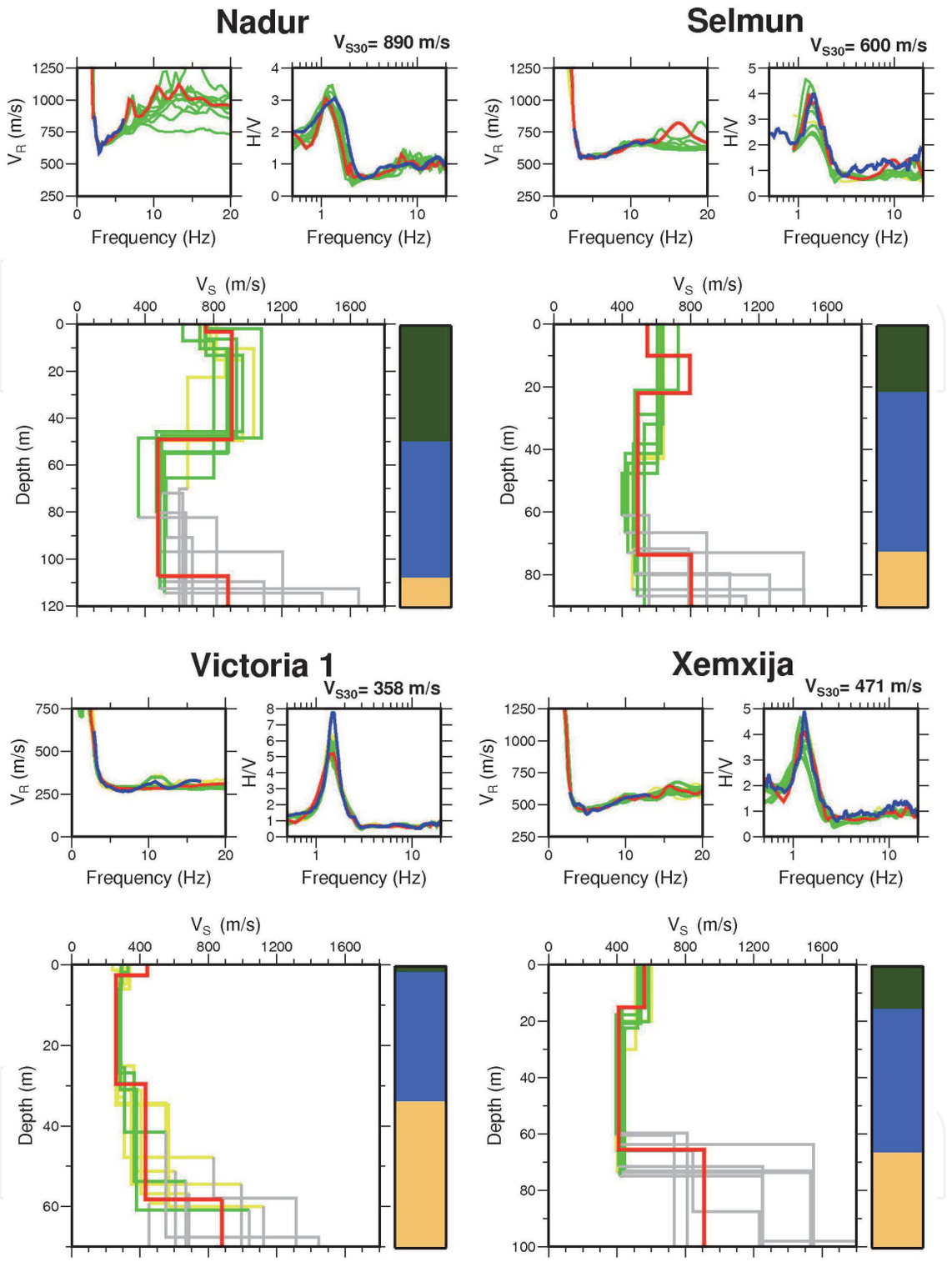

Figure 5.
The joint inversion results for Nadur, Selmun, Victoria 1 and Xemxija sites.

position and S-wave velocity of the low-velocity layer (the Blue Clay layer). Keeping in mind that broad exploration ranges were set in the parametrisations, such an agreement highlights the robustness of the inversion and the sensitivity of the curves to the presence and properties of the low-velocity layer. In addition, this justifies the use of global search methods, such as the GA, which are able to retrieve reasonable profiles without the need of an initial profile close to the solution.

This consistency between the models for a particular site diminishes in the prediction of the velocity of the UCL and more so of the GL layer, where, for example, values between 700 and 1800/s were obtained for the latter. This

inconsistency can be attributed to different facts such as the available array conditions, especially length and resonance frequency of geophones which limit the observable depth and the soft BC layer acting as a high-pass filter.

Lithotype	V_S range (m/s)
UCL	550–1100
BC	350–600
GL	700–1400

Table 1.
The V_S ranges for each lithotype obtained from all the studied sites.

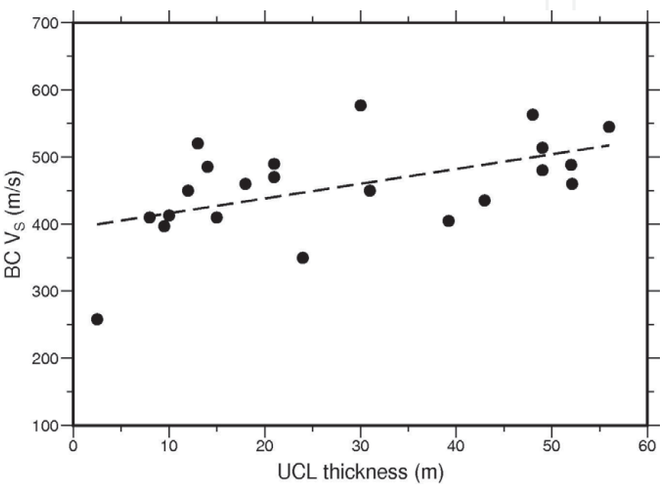

Figure 6.
A graph showing the variation of the BC shear-wave velocity with increasing UCL thickness.

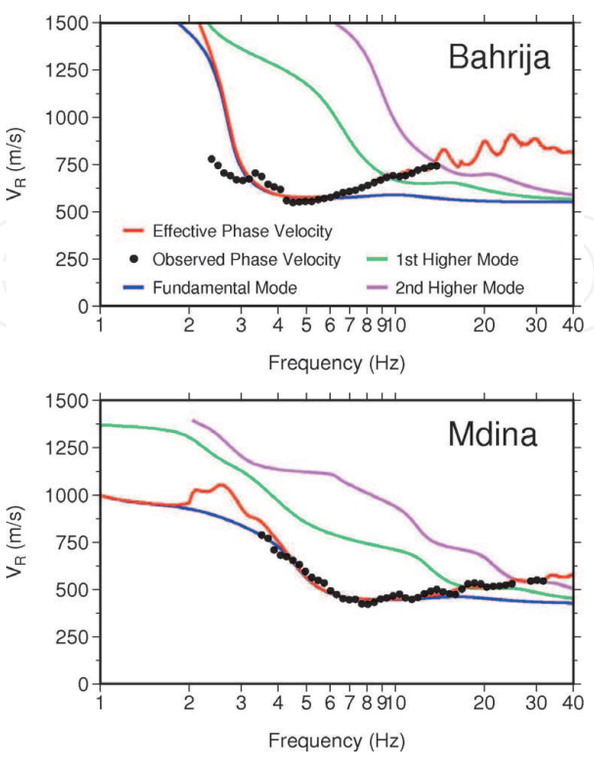

Figure 7.
Comparison of the observed Rayleigh-wave phase velocities (black dots) with the theoretical effective phase velocities and the first three Rayleigh-wave modes for the Bahrija and Mdina sites [11].

The obtained ranges for V_S and thickness for each layer from all the 20 tested sites are shown in **Table 1**. The V_S profiles reveal a variation in the shear-wave velocities of the geological layers at the different sites. Variations in the UCL shear-wave velocities are expected given the fact that the UCL exhibits considerable variation over the islands, ranging from very compact to highly fractured. The V_S in clay varies between 350 and 600 m/s which contrasts with values obtained at sites with outcropping BC layer (between 300 and 400 m/s) [12, 14]. **Figure 6** shows the variation of BC shear-wave velocity with thickness of the overlying UCL considering all the 20 profiles. A trend is clearly visible whereby the higher the thickness of the UCL layer, the higher the shear-wave velocity of the BC layer. This phenomenon can presumably be related to the overburden of the hard UCL layer on the BC, increasing the compactness of the particles, and thus the V_S of the layer.

Finally, in **Figure 7** we show the theoretical individual Rayleigh-wave dispersion curves up to the second higher mode for the best fit models compared with the observed effective dispersion curve for the Bahrija and Mdina models. The computed theoretical effective dispersion curve is also plotted and it can be observed that it fits very well with the observed data. These plots confirm that the effective Rayleigh mode is indeed the superposition of different modes with the higher modes playing an important role in the frequency range when this curve shows an inversely dispersive character [11].

4. Site-specific response analysis

Numerical site-specific response analysis was carried out using the equivalent-linear earthquake site response analysis programme SHAKE2000 [26]. The SHAKE2000 software computes the propagation of shear waves incident vertically on a package of horizontal layers, in which the wave-field in each layer is composed of upward and downward moving waves, whose amplitudes are dependent on the reflectivity/transmission matrices. The programme requires the following three main inputs:

- the soil layer properties (namely the V_S profile);
- the modulus reduction and damping curves for each material;
- the ground motion time-history including the layer number to which the input will be applied.

The V_S profiles obtained from the ambient noise measurements (**Figures 4**, 5 and **8**) were used as input for the soil layer properties for each site. The GL layer was chosen as the bedrock reference layer given that its velocity is generally more than 800 m/s. The modulus reduction and damping curves were chosen from the set of available curves within the package itself after consulting with local geotechnical experts. The chosen curves are displayed in **Figure 9**.

As for ground motion time-history, it is recommended that a suite of records is chosen which are compatible with the national seismic hazard parameters. From the probabilistic seismic hazard analysis conducted by [28], a plausible value for the mean peak ground acceleration (PGA) on rock sites corresponding to a 475-year return period is 0.08 *g*. [28] also note that from the study of historical seismicity and seismotectonic background it is indicated that the seismic hazard of the Maltese islands is related to both moderate magnitude events (M = 5.0–6.0) at short distances (d = 10–40 km) as well as high magnitude events (M = 6.5–8.0) at distances larger than 90 km. In this chapter, the far-field scenario of high magnitude events at

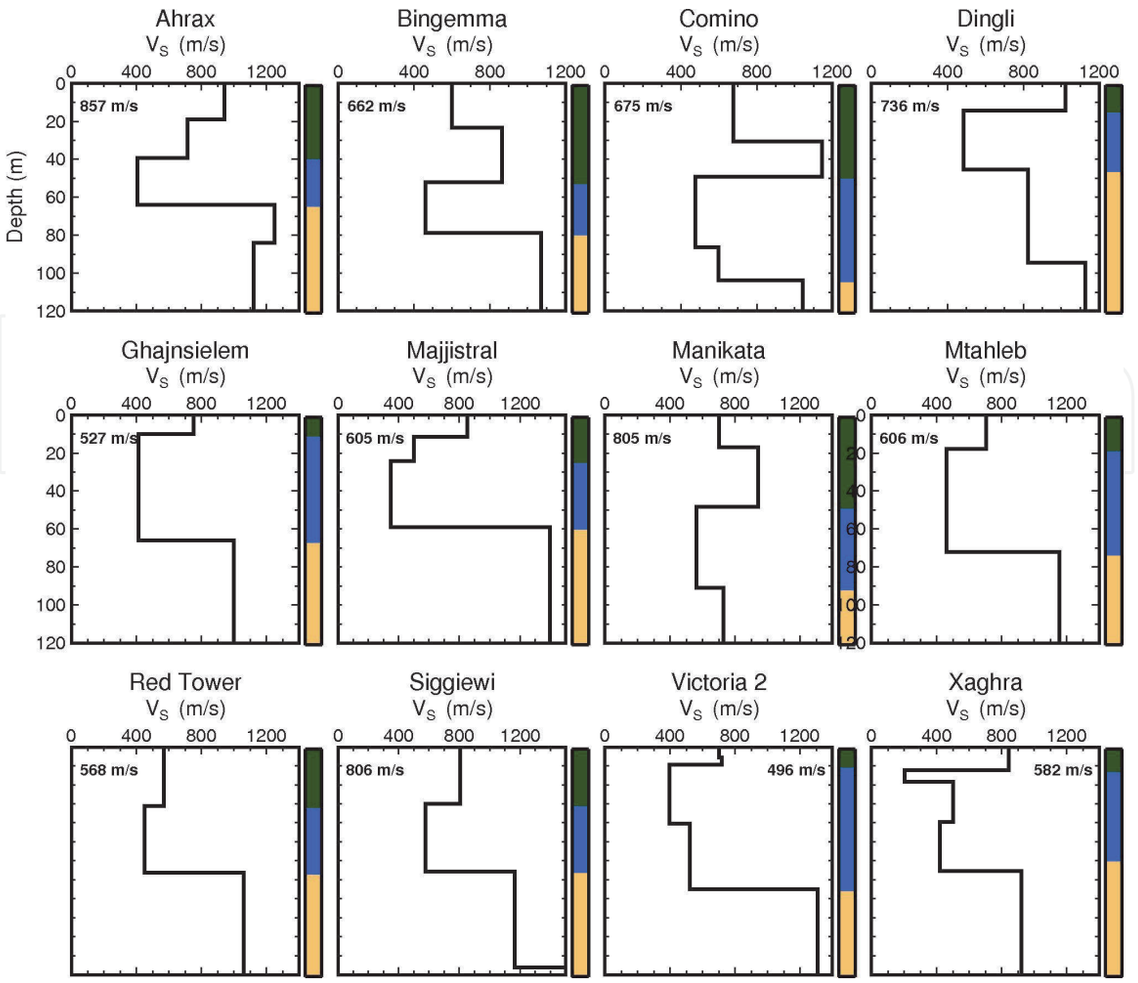

Figure 8.
*The best V_S profiles obtained for the 12 sites not shown in **Figures 4** and 5. The procedure of obtaining these profiles is the same as described in Section 3. The coloured bar represents a stratigraphical interpretation using the same colours as in **Figures 4** and 5.*

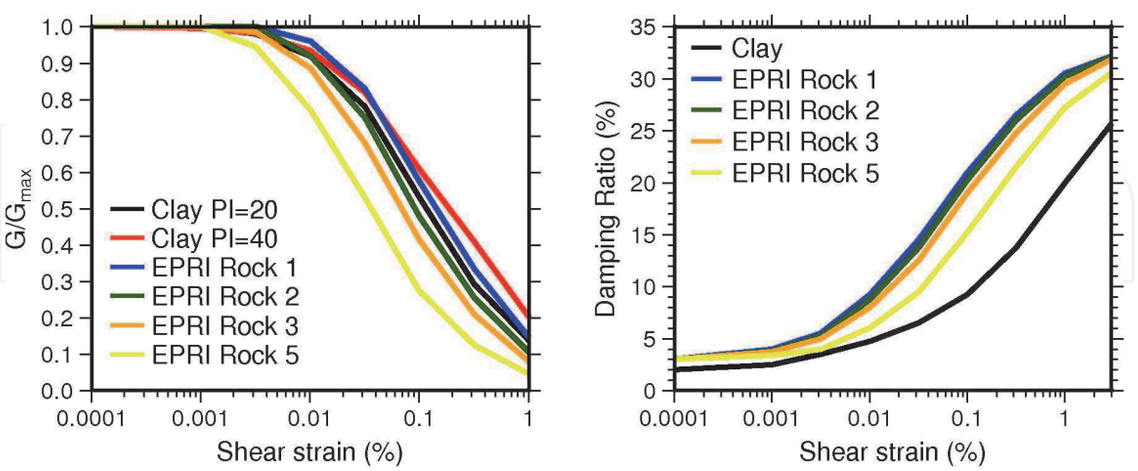

Figure 9.
The modulus reduction (left) and damping (right) curves used for the different layers in the simulation [27].

distances larger than 90 km will be presented considering that the worst case scenario earthquake which has hit the island was the 1693 M7.4 Sicily earthquake.

Since no real data of such earthquakes were ever recorded on the Maltese islands, the "spectrum matching" technique was used to find a suite of seven real accelerograms whose average spectra matched closely a chosen target spectrum. The REXEL code [29], which integrates the European Strong Motion Database, was

utilised for this purpose. The EC8 Type 1 spectrum, anchored at a PGA of 0.08 *g* was used as a reference spectrum and the lower and upper limit were set to 90% and 130% of the reference curve respectively (as recommended in the EC8). The search was conducted for magnitudes between 6.5 and 8.0 and distances between 60 and 200 km [28]. Only earthquake records at stations installed on class A sites, according to the EC8, were chosen. The possibility of scaling was allowed with a mean scaling factor not exceeding 5.

Plots of the scaled spectra of the chosen earthquakes together with the EC8 target spectra are presented in **Figure 10**. **Table 2** displays the information about the chosen suite of records.

All the required parameters were inputted in SHAKE2000 and the simulations were run. The software outputs various parameters however we will be focussing mainly on response spectra, PGA values and the theoretical transfer function.

4.1 The response spectra

The 5% damped elastic response spectra were grouped according to the corresponding EC8 site class (based on the V_{S30}) and are displayed in **Figure 11**. Considering the class A sites, it can be observed that all spectra demonstrate a higher response than the EC8 curve at periods longer than 0.5 s with Ahrax and

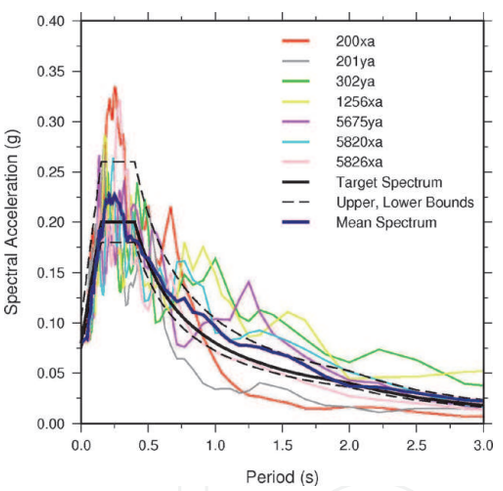

Figure 10.
The response spectra of the compatible combination of acceleration time-histories for the considered scenario. Event information is given in ***Table 2*** *[27].*

Code	Earthquake Name	Date	MW	Epicentral Distance (km)	Fault Mechanism	Scale Factor
200xa	Montenegro	15/04/1979	6.9	65	Thrust	0.36
201ya	Montenegro	15/04/1979	6.9	105	Thrust	1.07
302ya	Campano	23/11/1990	6.9	92	Normal	5.08
1256xa	Izmit	17/08/1999	7.6	92	Strike-slip	2.27
5675xa	Montenegro	15/04/1979	6.9	180	Thrust	3.67
5820ya	Strofades	18/11/1997	6.6	136	Oblique	0.87
5826xa	Strofades	18/11/1997	6.6	90	Oblique	1.21

Table 2.
Details of the chosen acceleration-time histories [27].

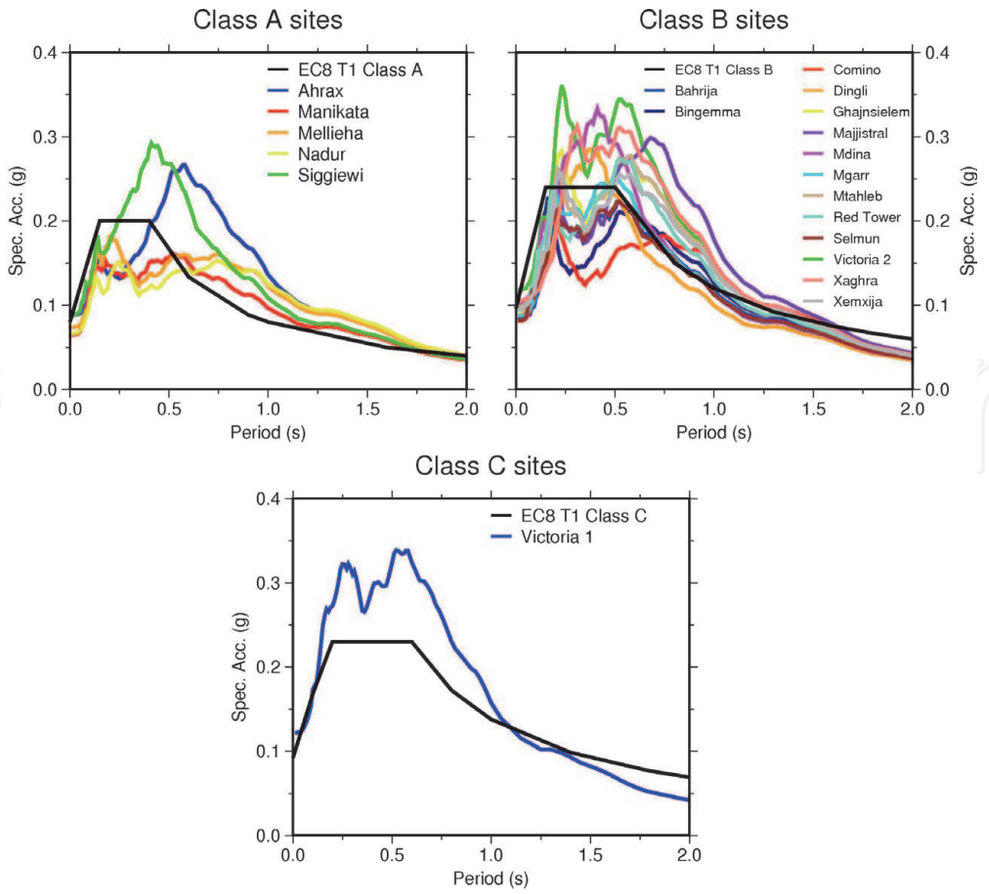

Figure 11.
The response spectra obtained at each site compared to the EC8 recommended site spectra.

Siggiewi showing a well-defined peak reaching up to 150% of the EC8 target spectrum for site class A. On the contrary, at shorter periods (less than 0.2 s), the majority of the sites lie below the EC8 target spectrum. The PGA (spectral acceleration at T = 0 s) is also lower than the EC8 target spectrum at almost all the sites. This behaviour is also similar for many of the Class B sites. As regards the class C site (Victoria 1, in Gozo), it is clear that the resulting spectrum is above the EC8 spectrum for a wide period range.

The behaviour highlighted here questions the V_{S30} criterion for site classification and its applicability in such geological settings especially in the context of the design of taller buildings that respond to higher periods of ground shaking.

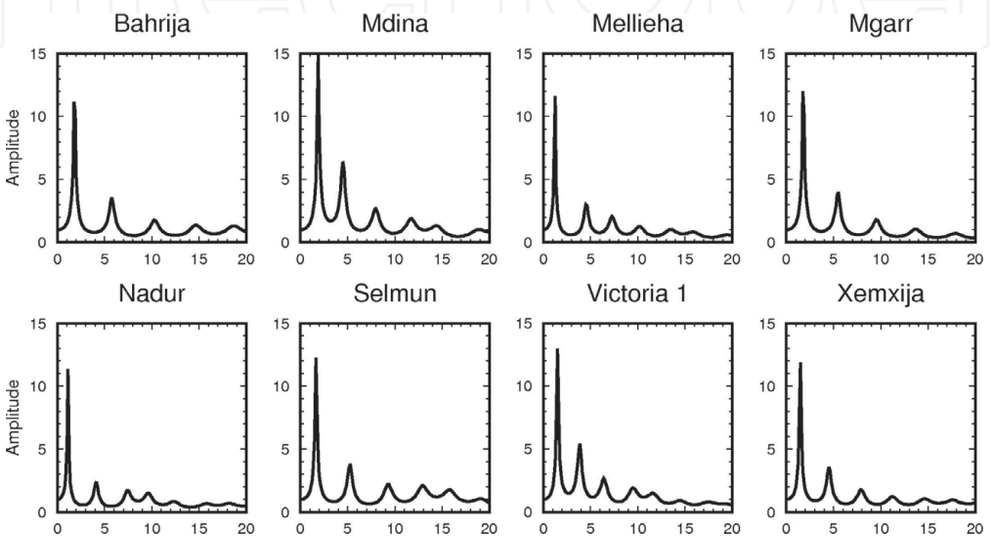

Figure 12.
The transfer functions of the eight sites chosen in Section 3.

Site	H/V peak Frequency (Hz)	Fundamental frequency (Hz)	Predominant period (s)/ Predominant frequency
Ahrax	1.5	1.63	0.58/1.72
Bahrija	1.25	1.75	0.52/1.92
Bingemma	1.47	1.5	0.16/6.25
Comino	0.94	1.25	0.14/7.14
Dingli	1.66	1.5	0.38/2.63
Ghajnsielem	1.34	1.5	0.23/4.35
Majjistral	1.22	1.38	0.68/1.47
Manikata	1.38	1.75	0.52/1.92
Mdina	1.84	1.88	0.41/2.44
Mellieha	1.38	1.25	0.21/4.76
Mgarr	1.75	1.75	0.52/1.92
Mtahleb	1.34	1.75	0.57/1.75
Nadur	1.38	1.13	0.74/1.35
Red Tower	1.41	1.63	0.52/1.92
Selmun	1.47	1.63	0.52/1.92
Siggiewi	1.50	2.13	0.41/2.44
Victoria 1	1.47	1.5	0.57/1.75
Victoria 2	1.41	1.63	0.23/4.35
Xaghra	1.31	1.5	0.31/3.23
Xemxija	1.31	1.5	0.23/4.35

Table 3.
The experimental H/V peak frequency, the fundamental frequency and the predominant period obtained for each study site [27].

Figure 12 shows the resulting transfer functions for the eight chosen sites in Section 3. The fundamental frequency obtained from the 1D transfer function (peak) and the H/V peak frequency obtained for all the sites are tabulated in **Table 3**. The predominant period, which is the period at which the response spectra (**Figure 11**) is the highest, is also tabulated. The fundamental frequencies obtained are in the range 1–2 Hz except for Siggiewi, for which a value slightly higher than 2 was obtained. These are in agreement with the values obtained using the H/V method. The resulting predominant periods range between 0.15 s and 0.75 s. Both the fundamental and predominant periods obtained fall in the range of resonance frequencies of typical 2–10 storey buildings [30, 31], which are becoming increasingly common in the northern part of the islands where the clay is present. Consequently, these buildings might suffer significant damage when this scenario is considered.

4.2 The amplification factors

In order to obtain a comparative measure of the amplification characteristics of different sites from the response spectra, the amplification factors F_{PGA}, FA and FV were calculated, as suggested by [32]. The amplification factors are defined as follows:

$$F_{PGA} = \frac{PGA_{output}}{PGA_{input}};$$

$$FA = \frac{SA_{output}}{SA_{input}};$$

$$FV = \frac{SV_{output}}{SV_{input}}$$

where the input values are obtained from the mean spectrum in **Figure 10** while the output values are obtained from the mean output spectra shown in **Figure 11**. *SA* and *SV* are obtained as follows:

$$SA = \frac{\int_{0.5TA}^{1.5TA} S_a \, dT}{TA}$$

where *TA* is the period at which the spectral acceleration (S_a) is maximum (also called the predominant period in Section 4.1 above); and

$$SV = \frac{\int_{0.8TV}^{1.2TV} S_v \, dT}{0.4TV}$$

with *TV* representing the period at which the velocity response spectrum (S_v) is maximum.

It can be noted that TA is generally smaller than TV, and that the integral in SA is generally determined over a range that includes shorter periods. In fact [33] deduce that FA is more relevant at shorter periods (< 0.5 s) while FV may be related to the behaviour at longer periods, and thus more relevant in the case of taller buildings. The values of F_{PGA}, FA and FV are mapped in **Figure 13**.

The F_{PGA} and FA values are in the majority of the cases both larger than 1 which implies that amplification is expected. However in a few cases values less than 1 were obtained, indicating that these sites are capable of deamplifying the input ground motion. F_{PGA} values are less than 1 at sites which are characterised by a UCL thickness greater than 48 m and are thus classified as class A according to the EC8

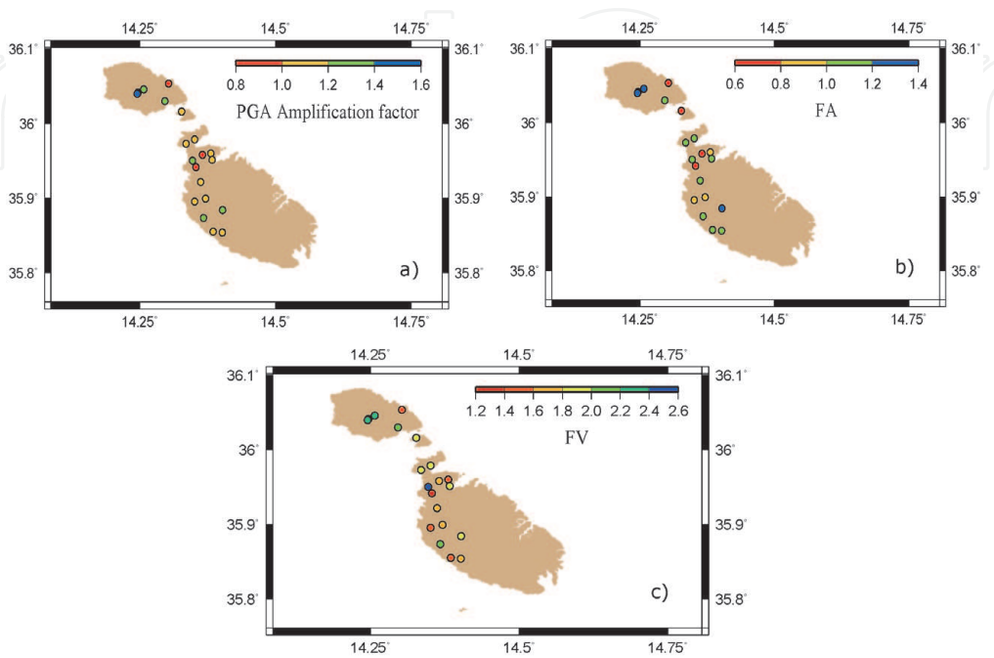

Figure 13.
Maps showing the three amplification factors at the studied sites: (a) F_{PGA}; (b) FA and (c) FV [27].

site classification. It is worth noting however that even though the Bingemma site is characterised by 52 m of UCL, the PGA is still slightly amplified. This could be due to the fact that the UCL is 'layered' into two strata with the upper layer having an average V_S of 600 m/s. In contrast, the highest F_{PGA} values were obtained for those sites where a thin layer of UCL limestone (less than 10 m) outcrops. This is also similar for the amplification factor FA.

In contrast, the amplification factor FV is greater than 1 at all sites, indicating that amplification is expected at longer periods. This is also in agreement with [33] where high FV amplification values were obtained for sites characterised by a low-velocity layer. In general, the same relationship was obtained for FA and FV: sites with thicker UCL exhibited lower amplification values. However, other characteristics of the V_S profiles also play an important role. For example, a higher FV value was obtained at the Majjistral site, which is characterised by a UCL thickness of 24 m, compared to sites which have a thinner UCL layer (e.g. Mdina which has a UCL thickness of 7 m). This could be interpreted as being due to the high impedance contrast (around 4) between the BC and GL layer at the Majjistral site.

To investigate possible correlations between the amplification factors and various parameters of the V_S profiles, the three amplification factors were plotted against: the thickness and V_S of the UCL and BC, the impedance contrast between the BC and underlying GL layer and the V_{S30}. The results are shown in **Figure 14**. The BC thickness exhibits no clear trend with any of the amplification factors. On the other hand, the FV values are seen to increase significantly with decreasing UCL thickness as well as with decreasing UCL and BC shear-wave velocities. These trends are also clear for F_{PGA} and FA, particularly with respect to BC shear-wave velocity. A clear trend can also be observed between FV and the impedance contrast, whereby the FV increases with impedance contrast. Lastly, the three amplification factors can be seen to decrease with an increase in V_{S30}. These observations highlight the role that the different properties which constitute the V_S profile play in site amplification and the difficulty in classifying the sites in rigid groups according to the properties of their upper 30 m of subsoil.

4.3 The in/adequacy of V_{S30}, $V_{Sbedrock}$ and site classification of building codes

Many authors [34, 35] have argued that the V_{S30} is not an adequate proxy to characterize the amplification potential of a site, especially in the type of geological situation being considered here. Since the low-velocity layer is found at a depth which is usually not considered in the V_{S30} calculation, these authors have suggested the use of the travel-time average shear-wave velocity down to the bedrock ($V_{Sbedrock}$) as an alternative.

To assess the reliability of the V_{S30} and $V_{Sbedrock}$ parameters and site classification schemes as proxies for site effects, a number of different shear-wave velocity profiles, all having the same V_{S30} (670 m/s +/− 15 m/s) and $V_{Sbedrock}$ (625 m/s +/− 15 m/s) were randomly constructed. According to the V_{S30} values, these profiles classify as EC8 Class B sites. Within the profiles, the shear-wave velocity and thickness of each layer (UCL, BC, UCL) were constrained to be within the ranges of values measured in the study, shown in **Table 1**. The numerical analysis was conducted again for each of these profiles and the resulting spectra for 4 such profiles, together with the Type 1 EC8 spectra for the different site classes, are presented in **Figure 15**.

Significant differences can be seen between the different response spectra at a wide period range. In particular, the PGA varies from 0.68 *g* to 0.1 *g* and the maximum spectral acceleration varies from 0.2 *g* to almost 0.35 *g*. As regards the EC8 design spectra, profile 2 is the only profile whose response is comparable with the EC8 site class B design spectrum. The spectrum of profile 4 can be compared

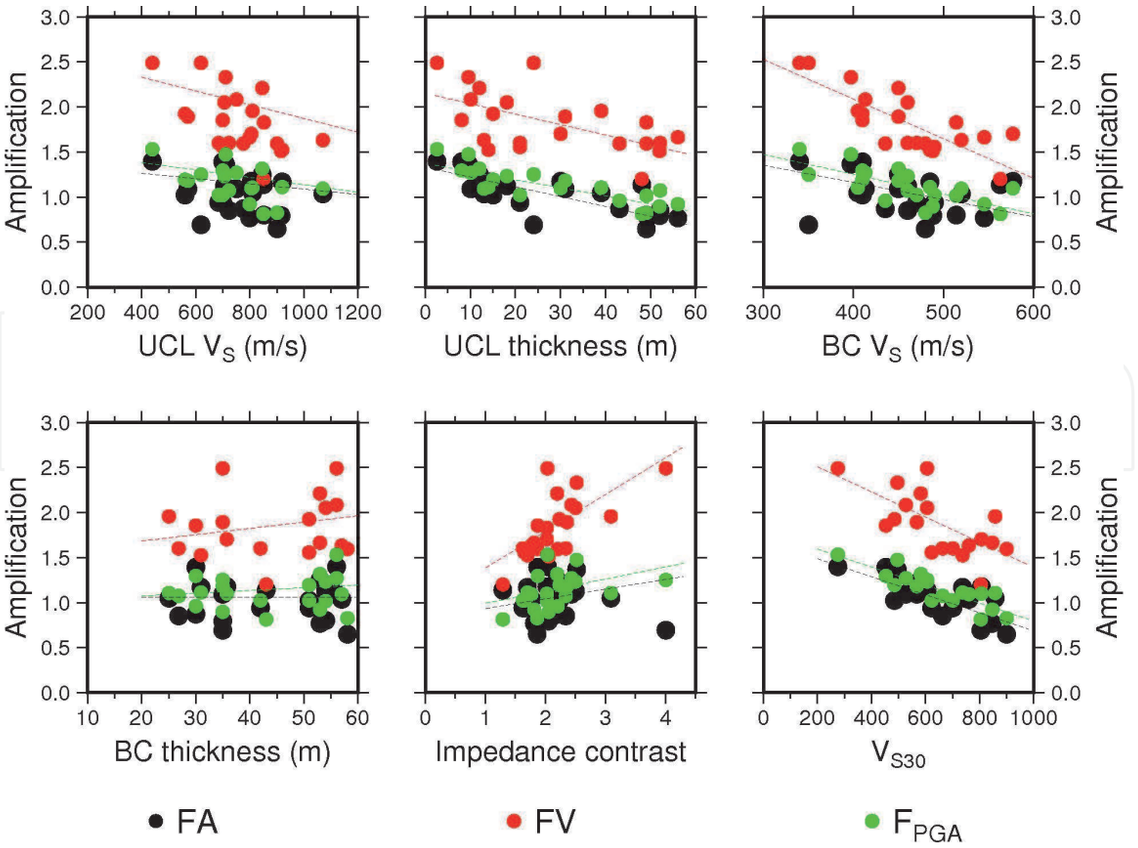

Figure 14.
Graphs showing the variation of the amplification factors with VS profile characteristics [27].

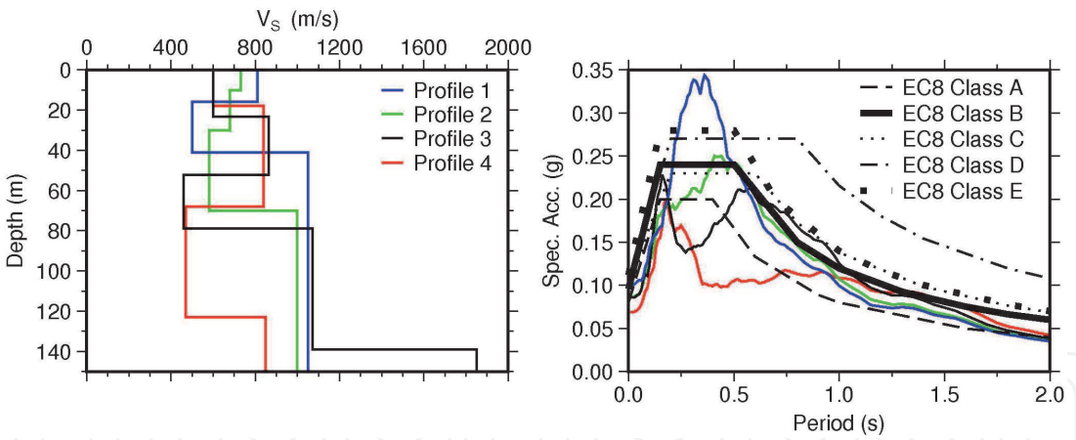

Figure 15.
Left: The hypothetical V_S profiles used for the test. Right: The resulting 5% damped response spectra of the used profiles and the EC8 design spectra.

with the site class A spectrum, profile 3 with site class C, while profile 1 can be seen to exceed the response of a class E site. These results imply that both the V_{S30} and $V_{Sbedrock}$ proxies are not the ideal parameters to use for site response approximations and neither is the use of rigid classes represented by one design spectrum. On the contrary, this continues to support the idea that site-specific response analysis is required, especially for sites characterised by a buried low-velocity layer.

5. Conclusion

Low-velocity layers are known to have the ability to amplify and lengthen the duration of earthquake ground motion. However, their effect when found buried

between two geologically harder layers is not well documented. The fact that the Maltese islands are characterized by a thick buried low-velocity layer in almost half of their span provides a good opportunity to study the effect of this type of stratigraphic sequence in a deeper manner. One of the main motivations for this study was the long-standing lack of knowledge within the local scientific and engineering community of how the present, highly densified building stock would fare in the case of a major earthquake in the region. However, the results from this study also provide an important contribution to the international seismological and earthquake engineering community.

A comprehensive investigation was carried out by obtaining V_S profiles at various sites around the islands which were then used as an input to the equivalent-linear site response analysis programme SHAKE2000. The H/V, ESAC and genetic inversion algorithm were used for obtaining V_S profiles at 20 sites and they have been shown to perform very well, particularly in resolving both the presence and the characteristics of a low-velocity layer in the stratigraphy.

The V_S profiles together with dynamic soil properties and design acceleration time histories were then used as inputs to SHAKE2000 to provide the acceleration response spectra at each site. Significant differences were obtained between the EC8 design spectra and some of the site response spectra at various periods. In particular, the response spectrum of the majority of the sites significantly exceeds the EC8 spectra at the plateau, and longer periods of the design spectrum for the site class based on V_{S30}. The predominant period and fundamental frequencies obtained from the transfer function coincide with resonance frequencies of typical 2–10 storey buildings, which are becoming increasingly common in areas where such stratigraphic sequence is present.

From the calculated amplification factors (F_{PGA}, FA and FV), it has been observed that sites with a thin capping of UCL above the clay layer exhibit high amplification factors. However, it was also noted that the other properties of the V_S profiles such as the impedance contrast also contribute to high FV amplification values.

Finally, the inadequacy of using V_{S30} or $V_{Sbedrock}$ to generalize the behaviour of different sites using one design response spectrum was shown by creating layered structures having the same V_{S30} and $V_{Sbedrock}$ but a different V_S profile. The resulting response spectra varied even by a factor of 2 or more at certain periods.

Whereas a site with outcropping clay is normally perceived as vulnerable within the local construction industry, sites on outcropping UCL may often be regarded as "rock sites" without adequate consideration of the effect of the underlying clay. The results here highlight the importance of carrying out site-specific response investigations in areas with buried low-velocity layers, and the need for care in the use of V_{S30} as a proxy for site amplification. The use of non-invasive ambient noise measurements allows a more cost-effective way of obtaining knowledge about the deeper V_S structure, which may influence earthquake response at the site.

Acknowledgements

This work was supported by the Endeavour Scholarship scheme financed out of Government of Malta national fund and also formed part of the SIMIT project (Integrated Italy-Malta Cross-Border System of Civil Protection) (B1-2.19/11) part-financed by the European Union under the ItaliaMalta Cross-Border Cooperation Programme, 2007–2013. The authors are grateful to Dr. D. Albarello and Dr. E.Lunedei for the use of the ESAC and joint inversion codes.

Author details

Daniela Farrugia*, Pauline Galea and Sebastiano D'Amico
University of Malta, Msida, Malta

*Address all correspondence to: daniela.farrugia@um.edu.mt

References

[1] Panzera F, Rigano R, Lombardo G, Cara F, Di Giulio G, Rovelli a. The role of alternating outcrops of sediments and basaltic lavas on seismic urban scenario: the study case of Catania, Italy. Bulletin of Earthquake Engineering. 2010;9(2): 411–439.

[2] Pilz M, Parolai S, Leyton F, Campos J, Zschau J. A comparison of site response techniques using earthquake data and ambient seismic noise analysis in the large urban areas of Santiago de Chile. Geophysical Journal International. 2009;178(2):713–728.

[3] Ansal A, Kurtuluş A, Tönük G. Seismic microzonation and earthquake damage scenarios for urban areas. Soil Dynamics and Earthquake Engineering. 2010;30(11):1319–1328.

[4] Tönük G, Ansal A, Kurtuluş A, Çetiner B. Site specific response analysis for performance based design earthquake characteristics. Bulletin of Earthquake Engineering. 2014;12(3): 1091–1105.

[5] Pedley, H. M., House, M. R., & Waugh, B. The geology of the Pelagian block: the Maltese Islands. The Ocean basins and margins. 1978;417–33.

[6] Zammit-Maempel, G.,. An Outline of Maltese Geology. Progress Press, Malta; 1977.

[7] Pedley M, Clarke MH, Galea P. Limestone Isles in a Crystal Sea. The geology of the Maltese islands. 2002.

[8] Gatt, P. Carbonate facies, depositional sequences and tectonostratigraphy of the Palaeogene Malta Platform [Doctoral dissertation]. Durham University; 2012.

[9] Magri O. A Geological and Geomorphological review of the Maltese Islands with special reference to the coastal zone. Territoris. 2006;6:7–26.

[10] Bard P-Y. Guidelines for the implementation of the H/V spectral ratio technique on ambient vibrations measurements, processing and interpretation. SESAME European research project WP-12-Deliverable D2312, European Commission – Research General Directorate Project No EVG1-CT-2000-00026 SESAME [Internet]. 2004;(December). Available from: ftp://ftp.geo.uib.no/pub/seismo/SOFTWARE/SESAME/USER-GUIDELINES/SESAME-HV-User-Guidelines.pdf

[11] Farrugia F., Paolucci E., D'Amico S., Galea P. Inversion of surface-wave data for subsurface shear-wave velocity profiles characterised by a thick buried low-velocity layer. Geophysical Journal International. 2016;206:1221–31.

[12] Vella A, Galea P, D'Amico S. Site frequency response characterisation of the Maltese islands based on ambient noise H/V ratios. Engineering Geology. 2013 Aug;163:89–100.

[13] Pace S. Shallow Shear Wave Velocity Structure in the Maltese Islands. Master's Thesis. 2012;

[14] Panzera F, D'Amico S, Galea P, Lombardo G, Gallipoli MR, Pace S. Geophysical measurements for site response investigation: preliminary results on the island of Malta. Bollettino di Geofisica Teorica ed Applicata. 2013; 54:111–128.

[15] Galea P, D'Amico S, Farrugia D. Dynamic characteristics of an active coastal spreading area using ambient noise measurements–Anchor Bay, Malta. Geophysical Journal International. 2014 Sep;199(2):1166–1175.

[16] Panzera F, Lombardo G. Seismic property characterization of lithotypes

cropping out in the Siracusa urban area, Italy. Engineering Geology. 2012;153: 12–24.

[17] Castellaro S, Mulargia F. The effect of velocity inversions on H/V. Pure and Applied Geophysics. 2009 Apr;166(4): 567–592.

[18] Di Giacomo D. Analysis and Modeling of HVSR in the Presence of a Velocity Inversion: The Case of Venosa, Italy. Bulletin of the Seismological Society of America. 2005 Dec;95(6): 2364–2372.

[19] Ohori M, Nobata A, Wakamatsu K. A Comparison of ESAC and FK Methods of Estimating Phase Velocity. Bulletin of the Seismological Society of America. 2002;92(6):2323–2332.

[20] Okada H. The Microtremor Survey Method. Tulsa, Oklahoma: Geophysical Monograph Series No. 12, Society of Exploration Geophysicists; 2003.

[21] Parolai S, Richwalski SM, Milkereit C, Fäh D. S-wave Velocity Profiles for Earthquake Engineering Purposes for the Cologne Area (Germany). Bulletin of Earthquake Engineering. 2006 Feb;4:65–94.

[22] Albarello D, Cesi C, Eulilli V, Guerrini F, Lunedei E, Paolucci E, et al. The contribution of the ambient vibration prospecting in seismic microzoning: an example from the area damaged by the April 6, 2009 L'Aquila (Italy) earthquake. Bollettino di Geofisica Teorica ed Applicata. 2011;52 (September):513–538.

[23] Tokimatsu K. Geotechnical site characterization using surface waves. Earthquake Geotechnical Engineering, Ishihara (ed). 1997;1333–1368.

[24] Arai H, Tokimatsu K. S-wave velocity profiling by joint inversion of microtremor dispersion curve and Horizontal-to-Vertical (H/V) spectrum. Bulletin of the Seismological Society of America. 2005 Oct;95(5):1766–1778.

[25] Picozzi M, Albarello D. Combining genetic and linearized algorithms for a two-step joint inversion of Rayleigh wave dispersion and H/V spectral ratio curves. Geophysical Journal International. 2007 Apr;169:189–200.

[26] Ordóñez GA. SHAKE2000 for the 1-D Analysis of Geotechnical Earthquake Engineering Problems User 's Manual.

[27] Farrugia, D., Galea, P., D'Amico, S. Modelling and assessment of earthquake ground response in areas characterised by a thick buried low-velocity layer. Natural Hazards. 2020;

[28] Panzera F, Longo E, Langer H, Lombardo G, Branca S. Site classification scheme for a complex geologic area : The study case of Mt . Etna. 2015;(November).

[29] Iervolino I, Galasso C, Cosenza E. REXEL: Computer aided record selection for code-based seismic structural analysis. Bulletin of Earthquake Engineering. 2010;8(2): 339–362.

[30] Galea, P., Micallef, T., Muscat, R., & D'Amico, S. Resonance frequency characteristics of buildings in Malta and Gozo using ambient vibrations. In: Georisks in the Mediterranean and their mitigation. 2015.

[31] Panzera, F., D'Amico, S., Lombardo, G., & Longo, E. Evaluation of building fundamental periods and effects of local geology on ground motion parameters in the Siracusa area, Italy. Journal of Seismology. 2016;20(3):1001–19.

[32] Working Group MS. Guidelines for seismic Microzonation. [Internet]. 2015. Available from: http://www.protezionecivile.gov.it/httpdocs/cms/attach_extra/GuidelinesForSeismicMicrozonation.pdf?

[33] Compagnoni M., Pergalani F., and Boncio P. Microzonation study in the Paganica-San Gregorio area affected by the April 6 , 2009 L'Aquila earthquake (Central Italy) and implications for the reconstruction. Bulletin of Earthquake Engineering. 2011;9:181–98.

[34] Pitilakis K, Riga E, Anastasiadis A. New code site classification, amplification factors and normalized response spectra based on a worldwide ground-motion database. Bulletin of Earthquake Engineering. 2013;11(4): 925–966.

[35] Gallipoli MR, Mucciarelli M. Comparison of Site Classification from VS30, VS10, and HVSR in Italy. Bulletin of the Seismological Society of America. 2009 Feb;99(1):340–351.